

# 1D optical lattice in a working MOT: co-existence of bound and free atoms diagnosed by the recoil-induced resonances

Maria Brzozowska, Tomasz M. Brzozowski, Jerzy Zachorowski, and Wojciech Gawlik  
*Marian Smoluchowski Institute of Physics, Jagiellonian University, Reymonta 4, PL 30-059 Cracow<sup>y</sup>*  
 (Dated: 9th February 2020)

We report on studies of simultaneous trapping of  $^{85}\text{Rb}$  atoms in a magneto-optical trap (MOT) and 1D optical lattice. Using Raman pump-probe spectroscopy, we observe the co-existence of two atomic fractions: the first, which consists of free, unbound atoms trapped in a MOT and the second, localized in the micropotentials of the optical lattice. We examine how the ratio of these two fractions and the shape of the lattice micropotentials change with the intensity of the MOT trapping beams.

PACS numbers: 32.80.Pj, 42.50.Vk, 42.65.-k

Optical lattices [1] constitute a convenient tool for studying phenomena related to periodically ordered systems. They are formed by the light-interference pattern, characterized by spatial, periodic light intensity and/or light polarization modulation. This modulation leads to periodically varying dipole force which, acting on the sufficiently cold atoms, can result in their localization in the minima or maxima of the light intensity map. Optical lattices with spatially modulated light polarization provide energy dissipation mechanisms resulting from cyclic optical pumping of the traveling atoms between their ground state sublevels [3]. This leads to atom temperatures below the Doppler cooling limit [4]. Usually, the optical lattices are filled with atoms either prepared in a MOT and further cooled in optical molasses or from the Bose-Einstein condensate [2]. In principle, stable lattice trapping can occur also in a MOT but this requires special beam configuration [5, 6].

We report on a 1D, blue-detuned optical lattice created directly in a regular working MOT, i.e. with fluctuating trapping fields constantly on. By means of the Raman pump-probe spectroscopy we study the co-existence of two atomic fractions: one, which is captured by the lattice, and the other, which is too hot to be localized in the lattice micropotentials. We also show that the depth of the lattice potential wells can be controlled by the MOT beams.

In our experiment (see Fig. 1) we use the  $^{85}\text{Rb}$  atoms trapped and cooled in a standard six-beam, vapor-loaded MOT [7]. Two additional beams intersect at a small angle in the trap center: the lattice standing wave and the running probe beam. Both have the same, linear polarization and are blue-detuned from the trapping transition  $^2S_{1=2} (F = 3) \rightarrow ^2P_{3=2} (F^0 = 4)$  by  $\Delta_{\text{latt}} = 2 \cdot 140 \text{ MHz} \cdot 23/3$ , where  $\Gamma$  denotes the natural linewidth. Such a detuning reduces resonant interaction with the atoms to a negligible level: the scattering rate does not exceed 44 kHz for the lattice beam intensities  $I_{\text{latt}} = 5 \cdot 35 \text{ mW/cm}^2$ . We have measured that such lattice intensities do not cause any visible heating. The trapping, probe and lattice beams are derived from diode

lasers injection-locked to a common master oscillator. The probe beam is scanned by 1 MHz around frequency  $\omega$  of the lattice beam and its transmission is monitored by the photodiode.

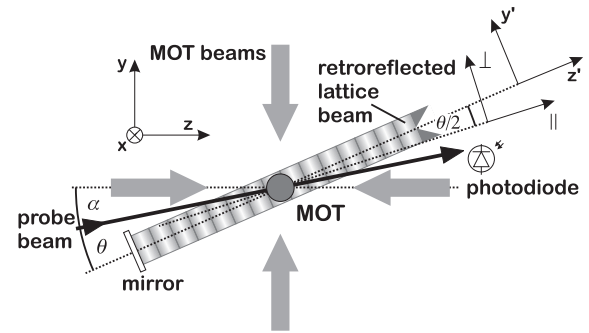


Figure 1: Layout of the experiment. The probe and retroreflected lattice beams intersect in a cloud of cold atoms in the working MOT. The momentum exchange due to Raman transitions involving the probe and the lattice photons is allowed in two directions:  $\hat{x}$  and  $\hat{y}$ . The 1D lattice constrains atomic motion along the  $z^0$  direction, which, for small  $\theta$ , nearly coincides with the  $\hat{y}$  direction. The third pair of the MOT beams and the MOT coils are not shown.

The probe and lattice beams drive Raman transitions with absorption of a photon from one beam followed by a stimulated emission to the second beam. The resulting change of atomic momentum  $\Delta \mathbf{p} = \hbar \mathbf{k} = 2\hbar k \hat{\mathbf{e}}_1 \sin \theta/2$ , where  $k$  is the modulus of the light wave vector,  $\theta$  is the angle between the beams, and  $\hat{\mathbf{e}}_1$  is the unit vector in the  $(y; z)$  plane, perpendicular to the bisector of  $\theta$  (Fig 2a). The sign in  $\Delta \mathbf{p}$  depends on the direction of the Raman process. Since the photons involved in the transition have the same polarization, the atom remains in the same ground state. Thus, the change of its momentum is accompanied only by the change of kinetic energy by  $\Delta E_{\text{kin}} = \hbar \Delta \mathbf{p} \cdot \mathbf{v}$  (Fig. 2b). The net variation of the probe beam intensity,  $s(\omega)$ , depends on the population difference of the momentum states and shows a resonant behavior around  $\omega = 0$  [8, 9]. This, so called, recoil-induced resonance, has a shape of the derivative of

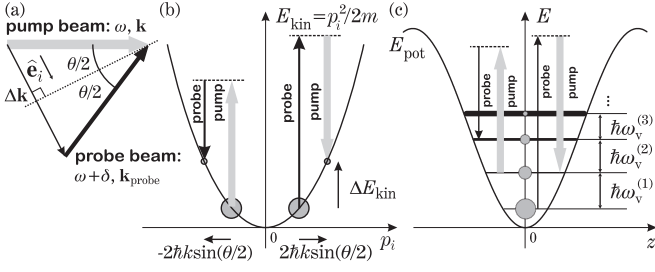


Figure 2: (a) Geometry of the light beams and momentum transfer  $\sim k$  in the Raman transition. (b) Raman transitions between kinetic states of free, unbound atoms. (c) Raman transitions between vibrational levels in the optical lattice potential. The vibrational levels spacing decreases due to anharmonicity. In (b) and (c) circles symbolize populations of the relevant levels.

the atomic kinetic momentum distribution along the momentum exchange direction,  $s(\delta) \propto \int \delta(p_i) \delta(p_i - \delta) dp_i$ , where  $p_i = p \cdot \hat{e}_i$ .

The above mechanism works for atoms which move freely and their kinetic energy can change in a continuous way but not for atoms trapped in optical lattices. In our case the motion of atoms confined in the 1D lattice wells becomes quantized in one direction. This results in vibrational structure of energy levels, unevenly spaced by  $\sim \hbar\omega_v^{(1)}, \sim \hbar\omega_v^{(2)}, \dots$  due to anharmonicity of the potential (Fig. 2c). Positions of the most distinct Raman vibrational resonances [10, 11], the first harmonic and overtone,  $\omega_v^{(1)}, \omega_v^{(2)}$ , associated with the change of vibrational quantum numbers by 1 and 2, can be found by averaging of vibrational level spacing over anharmonicity of the trapping potential with weights reflecting the temperature-dependent populations of given vibrational levels.

By changing intensities of the MOT and lattice beams, the atomic temperature and lattice depth can be varied so that a significant fraction of atoms may be localized in lattice wells. In our geometry of the probe and lattice beams three contributions are then expected in the probe transmission spectrum. Two of them are recoil-induced resonances: the narrow one, involving the probe and the nearly co-propagating lattice beam with  $p$  along the  $\hat{z}$  direction, and the wide one, for the probe and lattice beams nearly counter-propagating, with  $p$  along the  $\hat{y}$  direction (Fig. 1). The third possible contribution is the vibrational spectrum resulting from Raman transitions between quantized energy levels of the atoms trapped and oscillating in the 1D lattice micropotentials [10]. The spectra acquired in our experiment indeed exhibit all the expected contributions, as shown in Figs. 3b-d. It proves coexistence of two atomic fractions in a MOT: the unbound fraction of free moving atoms and the localized fraction of atoms captured by the 1D lattice. Thanks to large detuning  $\delta_{\text{latt}}$ , transitions involving the MOT-beams do not overlap with those induced by the lattice

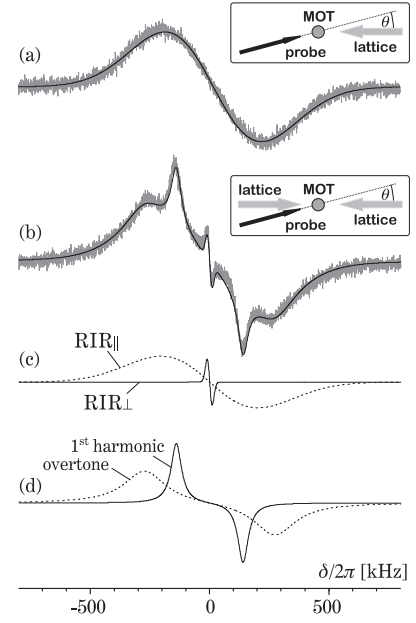


Figure 3: (a) Single, wide RIR spectrum acquired in the two-beam configuration shown in the inset. Solid line represents the fit by the first term of eq.(1). Such spectra are used to determine temperature of the atomic cloud. (b) Experimental spectrum (grey) recorded in the presence of the 1D optical lattice (inset) and the fit by eq.(1) (solid line). (c) RIR components of the fit: wide RIR associated with momentum exchange in the  $\hat{y}$  direction (dotted line) and narrow RIR associated with the exchange in the  $\hat{z}$  direction (solid line). (d) Vibrational components: first harmonic (solid line) and overtone (dotted line), extracted from the fit.

and probe beams. This is a significant simplification with respect to the previous work [12], allowing sensitive study of coexistence of the two fractions. By decreasing the intensity of the trapping beams, when the temperature of the magneto-optical trap was appropriately low, we studied modifications of the spectra indicating partition of our atomic sample into two fractions. The measured spectra were fitted with the equation

$$s(\delta) = A_{\text{jj}} \frac{\mathcal{G}(\delta; \text{jj})}{\mathcal{G}} + A_{\text{z}} \frac{\mathcal{G}(\delta; \text{z})}{\mathcal{G}} + L_{\text{I}} L(\delta; \omega_v^{(1)}; \Gamma) + L(\delta; \omega_v^{(1)}; \Gamma) + L_{\text{II}} L(\delta; \omega_v^{(2)}; \Gamma) + L(\delta; \omega_v^{(2)}; \Gamma); \quad (1)$$

where  $\mathcal{G}(\delta; \cdot)$  is the normalized Gaussian describing kinetic momentum distribution with standard deviation  $\sigma$ , and  $L(\delta; \omega; \Gamma)$  is the Lorentzian used for modeling the Raman vibrational resonance centered at  $\omega$  and with width  $\Gamma$ ;  $A_{\text{jj}}$  and  $A_{\text{z}}$  represent amplitudes of the wide ( $\text{jj}$ ) and narrow ( $\text{z}$ ) RIR contributions, and  $L_{\text{I}}$  and  $L_{\text{II}}$  are amplitudes of the vibrational resonances associated with the first harmonic and overtone [13]. Figs. 3c, d show separated recoil and vibrational contributions of expression (1) to the spectrum of Figs. 3b.

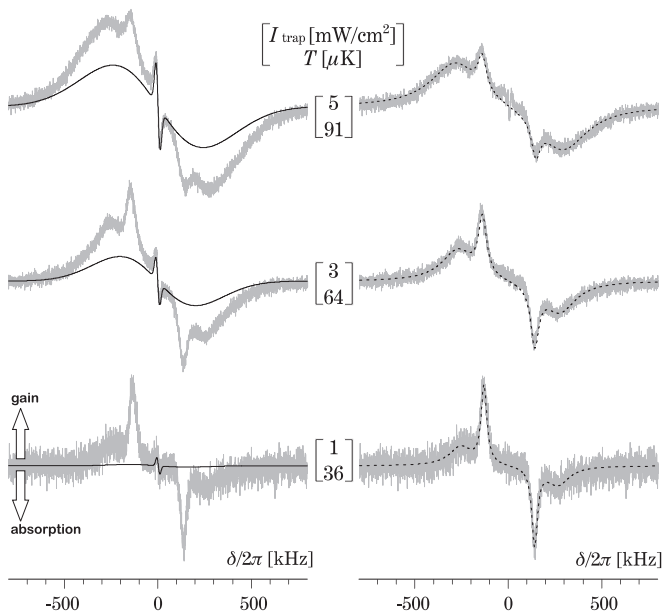


Figure 4: Probe transmission spectra with 1D optical lattice recorded for various MOT-beam intensities and related temperatures. Left column, measured spectra (grey) and RIR contributions (solid black) determined from two-beam thermometry (see text). Right column, vibrational contributions extracted by subtraction of RIR components from full spectra and theoretical fits (dotted).

In the spectra measured with three-beam configuration the first vibrational component is very distinct but the overtone overlaps with the wide RIR. To improve the fit accuracy, we reduced the number of free parameters by determining the temperature of the cold atomic cloud for each measurement. For that purpose, the mirror retroreflecting the lattice beam (Fig. 1) was blocked and the two-beam RIR velocimetry [14, 15] with the counter-propagating Raman beams was performed. In such a configuration, the only contribution to the spectrum is the wide RIR associated with the momentum transfer along the  $\hat{y}$  direction (Fig. 3a). Since our 1D optical lattice does not exhibit spatial polarization modulation, no additional cooling mechanism is present. Hence, we assume that the temperature of atoms in a MOT with and without the lattice is the same. Having determined the temperature  $T$ , we calculate the widths  $\hat{y}$  and  $\hat{z}$  [12, 14] and use them as constants in the fits with two first terms of eq. (1). The fitted RIR contributions are then subtracted from the spectra recorded with the lattice beams, i.e. with unblocked retroreflecting mirror of Fig. 1. The resulting difference constitutes pure lattice contribution which is very well reproduced by the last terms of eq. (1), as seen in Fig. 4.

For decreasing temperature of the atomic cloud we observed increase of the amplitude of the vibrational contribution relative to the RIR contribution. This indicates a growth of the fraction localized in the 1D optical lattice.

We also observed systematic variation of the relative amplitudes of the two RIR contributions. As it can be seen in Fig. 4, for lower temperatures the amplitude of the wide RIR associated with the momentum exchange in the  $\hat{y}$  direction is noticeably smaller than for the  $\hat{z}$  direction. This behavior can be explained by constraints imposed by 1D optical lattice on the atomic movement and consequent suppression of recoil in the  $\hat{y}$  direction. Hence, localized atoms do not contribute to the wide RIR. Since the fraction of atoms trapped in the lattice grows with the decrease of temperature at the expense of unbound atoms, the amplitude of the wide RIR becomes smaller. Inversely, since there is no lattice trapping in the  $\hat{z}$  direction, the localization does not affect the narrow RIR.

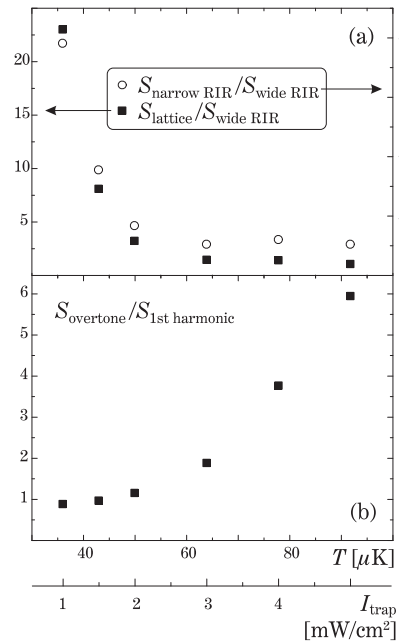


Figure 5: Trap-beam intensity and temperature dependence of the atomic fractions estimated by calculating areas  $S$  under relevant spectra contributions: (a)  $S_{\text{lattice}}=S_{\text{wide RIR}}$ , the ratio of the localized and unbound atomic fraction and  $S_{\text{narrow RIR}}=S_{\text{wide RIR}}$  re-scaled as described in text, the ratio of number of atoms moving free in the  $\hat{z}$  and  $\hat{y}$  directions, (b)  $S_{\text{overtone}}=S_{\text{1st harmonic}}$ , the ratio of atoms undergoing Raman transitions responsible for the 1<sup>st</sup> harmonic and overtone.

To estimate the relative contributions of the discussed atomic fractions, we numerically evaluated areas  $S$  under relevant terms of eq. (1). Fig. 5a presents the calculated ratio  $S_{\text{lattice}}=S_{\text{wide RIR}}$ , which represents the temperature dependence of the relative number of atoms in the lattice to the atoms that move free in the  $\hat{y}$  direction. Fig. 5a depicts also the ratio  $S_{\text{narrow RIR}}=S_{\text{wide RIR}}$  re-scaled by a geometrical factor  $\sin(\theta)=\sin[(180-\theta)/2]$  [12, 14]. As the transition amplitudes for both RIRs are the same, the ratio can be straightforwardly treated as the relative number of the atoms unbound in the  $\hat{z}$  and  $\hat{y}$  directions. The two plots in Fig. 5a exhibit sim-

ilar character resulting from increase of the unbound atomic fraction with growing temperature. As expected,  $S_{\text{narrow RIR}} = S_{\text{wide RIR}}$  asymptotically tends to unity. For higher temperatures and trapping-beam intensities we observed the systematic increase of the overtone contribution relative to the 1<sup>st</sup> harmonic ( $S_{\text{overtone}} = S_{1^{\text{st}} \text{ harmonic}}$  ratio, depicted in Fig. 5b). We attribute it to the rising probability of the overtone transitions due to higher anharmonicity of the lattice potential for higher trapping-beam intensity [16].

We have also studied a change of the position of the average first harmonic frequency,  $\nu^{\text{I}}$ , with the increase of temperature at higher trapping-beam intensity (Fig. 6). As the higher vibrational levels become more populated with the increasing temperature, one might expect a shift of the vibrational resonances towards lower frequencies. However,  $\nu^{\text{I}}$  increases when the trapping light becomes more intense. We interpret this effect as follows. The levels of the atoms in a MOT with the lattice beams switched on are light-shifted by two fields: the red-detuned MOT field and the blue-detuned lattice field. When the intensity of the trapping light is increased, the light-shifts of the ground atomic sublevels also increase. This leads to smaller detuning of the atomic resonance frequency relative to the blue-detuned lattice beam. Since the depth of the lattice potential  $U_{\text{latt}}$  is proportional to  $I_{\text{latt}} = I_{\text{trapp}}$ , we observe the increase of  $U_{\text{latt}}$  followed by increase of  $\nu^{\text{I}} / \sqrt{U_{\text{latt}}}$ . The calculations based on such simplistic explanation, despite the qualitative agreement, fail to reproduce the observed dependence of  $\nu^{\text{I}}$ . It indicates that in our case bichromatic dressing [17] cannot be reduced to independent light shifts. The observed phenomenon suggests a practical way of adjusting the lattice potential by an additional light field that is not directly associated with creation of the lattice.

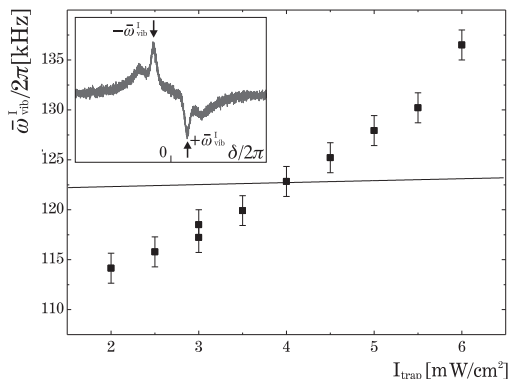


Figure 6: Frequency  $\nu^{\text{I}}$  of the vibrational resonance (marked by arrows on the lattice spectrum in the inset) as a function of the MOT trapping beams intensity. Solid line presents the independent light-shift prediction. Although it shows the correct rising slope, it does not reproduce the magnitude of experimental shifts.

In conclusion, we have realized a stable 1D optical lattice created directly within a working MOT. The lattice can capture relatively hot atoms ( $\sim 100$  K).

By performing Raman pump-probe spectroscopy we investigated the co-existence of the two atomic fractions: one trapped in a lattice and the other moving freely in the magneto-optical trap. We demonstrated that the suppression of recoil along lattice-trapping directions makes it possible to use the recoil-induced resonances as a tool for studying the dynamics of the lattice loading. In this way we extended the scope of the RIR, usually applied for direction-selective velocimetry [8, 12, 14, 15]. Moreover, we found that the trapping beams significantly affect the lattice potential. This opens a possibility of controlling the optical lattice properties by independent light fields.

This work is supported by the Polish Ministry of Science and Information Society Technologies and is part of a general program on cold-atom physics of the National Laboratory of AMO Physics in Toruń, Poland. We would like to thank Julien Saby for his assistance in analysis of the experimental data and to Dmitry Budker for his remarks on the manuscript.

Electronic address: gawlik@uj.edu.pl

URL: <http://www.if.uj.edu.pl/ZF/qnog/>

- [1] for review see, for example, G. Grynberg and C. Robillard, Phys. Rep. **355**, 335 (2001) and references therein.
- [2] see, for example, M. Greiner, I. Bloch, O. Mandel, T.W. Hänsch and T. Esslinger, Appl. Phys. B **73**, 769-772 (2001) and references therein.
- [3] J. Dalibard and C. Cohen-Tannoudji, J. Opt. Soc. Am. B **6**, 2023 (1998).
- [4] P.D. Lett, R.N. Watts, C.I. Westbrook, W.D. Phillips, P.L. Gould and H.J. Metcalf, Phys. Rev. Lett. **61**, 169 (1988).
- [5] K.I. Petsas, A.B. Coates and G. Grynberg, Phys. Rev. A, **50**, 5173 (1994).
- [6] H. Schadwinkel, U. Reiter, V. Gomer and D. Meschede, Phys. Rev. A, **61** 013409 (1999).
- [7] E. L. Raab, M. Prentiss, A. Cable, S. Chu, and D. E. Pritchard, Phys. Rev. Lett. **59**, 2631 (1987).
- [8] G. Grynberg, J.-Y. Courtois, B. Lounis, and P. Verkerk, Phys. Rev. Lett. **72**, 3017 (1994).
- [9] P. Verkerk, Proceedings of The International School of Physics, Varenna, **Course CXXXI**, 325 (1996).
- [10] P. Verkerk, B. Lounis, C. Salomon, and C. Cohen-Tannoudji, J.-Y. Courtois and G. Grynberg, Phys. Rev. Lett. **68**, 3861, (1992).
- [11] P.S. Jessen, C. Gerz, P.D. Lett, W.D. Phillips, S.L. Rolston, R.J.C. Spreeuw, and C.I. Westbrook, Phys. Rev. Lett., **69** 49 (1992).
- [12] T. M. Brzozowski, M. Brzozowska, J. Zachorowski, M. Zawada, and W. Gawlik, Phys. Rev. A **71**, 013401 (2005).
- [13] Our calculations based on Ref. [18] proved that higher overtones can be neglected.
- [14] M. Brzozowska, T.M. Brzozowski, J. Zachorowski and W. Gawlik, *submitted*.

- [15] D. R. Meacher, D. Boiron, H. Metcalf, C. Salomon, and G. Grynberg, *Phys. Rev. A* **50**, R1992 (1994).
- [16] G. Herzberg, *Molecular Spectra and Molecular Structure*, Krieger Publishing Company 1992, pp.85-88
- [17] e.g. Z. Ficek and H.S. Freedhoff, *Phys. Rev. A*, **48** 3092 (1993).
- [18] C. Cohen-Tannoudji, J. Dupont-Roc and G. Grynberg, *Atom-Photon Interactions: Basic Processes and Applications*, John Wiley & Sons, 1992, pp. **86-87**; **519-523**.